4620

CNN based Super-Resolution of Intravoxel Incoherent Motion Imaging for Liver

Jiqing Huang[1], Jin Qin[1], Lihui Wang[1], Rongpin Wang[2], Zi-Xiang Kuai[3], Chen Ye[1], Tianye Wang[1], and Yuemin Zhu[4]

[1]Key Laboratory of Intelligent Medical Image Analysis and Precise Diagnosis of Guizhou Province, School of Com-pute Science and Technology, Guizhou University, Guiyang, China, [2]Department of Radiology, Guizhou Provincial People's Hospital, Guiyang, China, [3]Harbin Medical University Cancer Hospital, Harbin, China, [4]Univ.Lyon, INSA-Lyon, Université Claude Bernard Lyon 1, UJM-Saint Etienne, CNRS, Inserm, CREATIS UMR 5220, U1206, F-69621, LYON, France

Synopsis

We investigated the super-resolution reconstruction method for IVIM imaging based on convolution neural networks (CNN). Three-layers-CNN was constructed and trained firstly with a series of paired low- and high-resolution images, and then the super-resolution IVIM images were reconstructed with such network, the reconstruction quality was evaluated finally in terms of PSNR, SSIM, diffusivity, perfusion fraction and pseudo-diffusivity respectively. The results show that the CNN-based super resolution reconstruction for IVIM has a great performance and may enable IVIM to be analyzed with unprecedent resolution.

INTRODUCTION

Intravoxel incoherent motion (IVIM) imaging is currently a promising technique to reveal the micro changes of tissue pathophysiology by detecting both diffusion and pseudo perfusion information[1,2]. However, such microscopic parameters were estimated usually at a relatively macroscopic scale (voxel size is in millimeters). Increasing the imaging spatial resolution is fundamental for improving the estimation accuracy but at expense of long acquisition time which will result in the degradation of image quality caused by the motion of patient[3]. To cope with this issue, a reliable super-resolution (SR) image reconstruction method for IVIM based on convolu-tional neuro network (CNN) was proposed in this work.

METHODS

The diffusion weighted (DW) images for liver of a healthy volunteer were acquired with the multiple *b* values (*b* = 0, 3, 5, 10, 15, 20, 25, 30, 40, 50, 75, 100, 200, 400, 600 and 800 s/mm^2) with a 3T Philips MRI system. The in-plane resolution of DW image is 1.56 ×1.56 mm^2 and the slice thickness is 6 mm. For obtaining the super-resolution DW images, a three layers CNN was constructed. The original low-resolution (LR) images were firstly enlarged to the target size by bicubic interpolation and considered as the initial input of CNN. In the first layer, 64 convolution kernels with size of 9×9 was used to extract the image feature maps. In the second layer, 32 non-negative filters (the output of the filter must be positive or zero) with size of 1×1 were used to form representations of high-resolution (HR) image patches. These patches were weighted averaged in the third layer using a convolution filter of size 5×5 to achieve the final super-resolution reconstruction result. The parameters of kernels used in CNN were trained by a series of paired HR images and LR images. The minimum mean square error(MMSE) between the reconstructed and original HR images were used as the loss function, which was minimized using stochastic gradient descent optimization method with a learning rate of 10^{-4} for the first two layers and 10^{-5} for the last layer.

After the reconstruction, biexponential intravoxel incoherent motion analysis was performed to extract diffusivity (*D*), perfusion fraction (*f*), and pseudo-diffusivity (D^*). The peak signal to noise ratio (PSNR), signal to noise ratio (SNR) and structure similarity (SSIM) of the reconstructed and original HR images was calculated, and *D*, *f* and D^* at different scales were compared quantitatively.

RESULTS

SR image reconstruction was performed for all DW images with different *b* values. In Fig.1 were only illustrated the reconstruction results for DW image with *b*=0. The LR image was generated with a down sampling ratio of 2, as shown in Fig.1(a), the original and reconstructed HR images were given respectively in Fig.1(b) and Fig.1(c), the SR image which twice the original image resolution was demonstrated in Fig.1(d). The image quality was obviously improved.

The error between the original and the reconstructed HR images for different *b* values, expressed by PSNR, SNR, and SSIM was given in Table.1. We observed that mean PSNR for DW images of all the b values is about 41 dB, the mean SNR of that is higher than 20dB, and the SIMM is up to 0.98, which are better than most of other works.[4,5]

The IVIM parameters, including diffusivity, pseudo-diffusivity, and perfusion fraction of the region of interest (ROI), underlined with yellow boundary in Fig.1, were also calculated using nonlinear least square fitting algorithm, as shown in Fig.2. The corresponding statistics was given in Fig.3. For visualizing these parameters in the same figure, the mean ± std of diffusivity and perfusion fraction were timed by 100.

We observed that the mean ± std of the diffusivity and the perfusion fraction did not change too much with the variation of spatial resolutions, however, the mean ± std of pseudo-diffusivity decreased a little as the resolution of image increased. The parameters for the original HR images and that for the reconstructed HR images were almost the same, which validated further our super resolution reconstruction method.

Discussion

SR technique is of great interest for medical imaging since it overcomes the limit of hardware. To our knowledge, it is the first time to perform SR in IVIM, with the current scanner, it enables us to evaluate the microscopic diffusion and perfusion information at a high spatial resolution and correspondingly improve the estimation accuracy.

Conclusion

We have proposed a novel SR method for IVIM based on CNN networks, it has been shown that such SR technique performs very well in the reconstruction of DW images and the diffusion and perfusion parameters.

Acknowledgements

This work was supported by the National Nature Science Foundations of China (Grant No. 61661010, 61562009, 81701654), the Funds for Talents of Guizhou University (No. 2013(33)), the Nature Science Foundation of Guizhou province (Qiankehe J No.20152044, 20157115, 20161069) and the French ANR (under MOSIFAH ANR-13-MONU-0009-01).

References

1. Li L, Xie Y, Hu W, Zhang W. Neurocomputing Single image super-resolution using combined total variation regularization by split Bregman Iteration. Neurocomputing. 2014;142:551-560.

2. Chiaradia M, Baranes L, Nhieu JT, et al. Intravoxel incoherent motion (IVIM) MR imaging of colorectal liver metastases: are we only looking at tumor necrosis? J Magn Reson Imaging. 2014;39(2):317-325.

3. Plenge E, Poot DHJ, Bernsen M, et al. Super-resolution methods in MRI: Can they improve the trade-off between resolution, signal-to-noise ratio, and acquisition time? Magn Reson Med. 2012;68(6):1983-1993.

4. Coupé P, Manjón J V, Chamberland M, Descoteaux M, Hiba B. Collaborative patch-based super-resolution for diffusion-weighted images. Neuroimage. 2013;83:245-261.

5. Shi F, Cheng J, Wang L, Yap P-T, Shen D. Super-Resolution Reconstruction of Diffusion-Weighted Images Using 4D Low-Rank and Total Variation BT - Computational Diffusion MRI: MICCAI Workshop, Munich, Germany, October 9th, 2015. In: Fuster A, Ghosh A, Kaden E, Rathi Y, Reisert M, eds. Cham: Springer International Publishing; 2016:15-25.

Figures

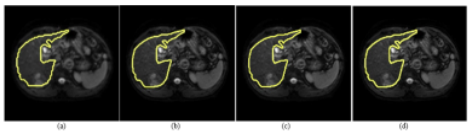

Fig.1 DW images with different spatial resolutions. (a) LR image generated by down-sampling with a ratio of 2, (b) Original DW image considered as the ground truth of HR image, (c) reconstructed HR image, (d) Reconstructed super-resolution image

b (s/mm2)	0	3	5	10	15	20	25	30	40	50	75	100	200	400	600	800
PSNR/dB	40.1	40.7	41.4	41.4	41.8	42.2	42.2	41.4	40.8	40.9	41.2	42.5	38.5	39.7	40.7	41.1
SNR/dB	21.0	20.8	21.0	20.8	21.4	20.9	22.4	21.0	21.6	21.8	21.7	22.0	22.9	23.0	25.4	24.4
SSIM	0.98	0.98	0.98	0.98	0.98	0.98	0.98	0.98	0.98	0.98	0.98	0.98	0.97	0.98	0.98	0.98

Table.1 PSNR SNR and SSIM for the sixteen SR image experiments

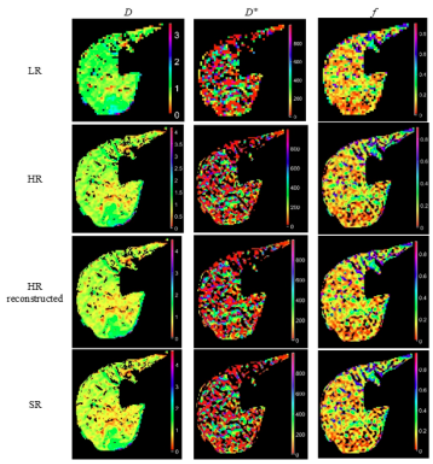

Fig.2 D, D* and f maps of IVIM obtained with different spatial resolutions

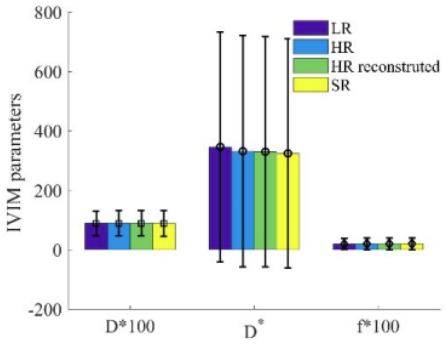

Fig. 3 Mean ± std of IVIM parameters obtained with different spatial resolutions

Proc. Intl. Soc. Mag. Reson. Med. 26 (2018)
4620